JOURNAL OF AEROSPACE COMPUTING, INFORMATION, AND COMMUNICATION
Vol. 5, September 2008

Investigating Time-Delay Effects for Multivehicle Formation Control

Lesley A. Weitz* and John E. Hurtado†
Texas A&M University, College Station, Texas 77843-3141

DOI: 10.2514/1.34740

Advances in communication, navigation, and computational systems have enabled greater autonomy in multivehicle systems. However, time-delay effects owing to measurement, actuation, communication, or operator delays are introduced as system complexity increases. In this paper, a straightforward method is presented to determine the maximum allowable time delays for a linear, n-dimensional system. Delay differential equations are one method to model systems with delay, and the theory presented here is based upon well-known stability results for a scalar, first-order delay differential equation. Modal-coordinate transformations are used to diagonalize, and thus, decouple closed-loop equations of motion to which the scalar, first-order delay-differential-equation results are applied in order to find optimal bounds on the time delay. Hence, stability bounds for a given closed-loop control form can be determined by solving an eigenvalue problem, which is a departure from other delay-differential-equation results that require solutions to linear matrix inequalities or a problem-specific Lyapunov function to prove stability. This theoretical development is applied to a formation-control problem with five vehicles. Control laws are developed for the vehicle formation using two different communication structures: leader–follower and bidirectional. Simulation results are used to demonstrate formation convergence, and robustness of the formations to time-delay effects are discussed.

I. Introduction

THE design and implementation of decentralized, cooperative controllers for multivehicle systems will enable greater autonomy and task efficiency for a wide range of engineering applications. Decentralized systems have distributed control authority between individual entities rather than a single central authority that calculates control inputs for all entities. In a cooperative control scheme, individual vehicles share state and environmental information with other vehicles in order to determine the control inputs that will achieve a common objective. Applications of these control concepts include the development of automated highway systems [1–4], next-generation air traffic management systems [5–8], and unmanned aerial vehicle (UAV) systems [9–12]. Whereas decentralized systems are more robust to communication failures and structural reconfigurations[13], the impact of intervehicle communication delays on system stability and performance must also be considered.

Stability analysis of systems with delay is an important aspect to the design and control of decentralized systems. In particular, complex systems are subject to measurement, actuation, communication, and human-operator

Received 23 September 2007; revision received 8 April 2008; accepted for publication 10 April 2008.
* Graduate Student, Department of Aerospace Engineering; lweitz@tamu.edu; Member AIAA.
† Associate Professor, Department of Aerospace Engineering; jehurtado@tamu.edu; Senior Member AIAA.

delays, and in many cases it is necessary to take these delays into account when designing control laws. Olfati-Saber and Murray investigated control laws with time-delayed feedback for dynamic agents using graph theory[14], and Subbarao and Muralidhar have approached the communication-delay problem for UAVs by designing a nonlinear multi-input/multi-output (MIMO) state observer with output delays[15]. Much of the literature on multivehicle control does not directly address time-delay effects in feedback delays; for example, Dionne and Rabbath have included communication delays in simulations, but these delay effects were not incorporated into the control design[16].

This research considers an approach to quantify stable time delays in the feedback states of decentralized, cooperative control laws. The research objective was to evaluate the maximum allowable delay for stability using delay differential equations (DDEs) to model the n-dimensional closed-loop systems with delayed feedback. A common coordinate transformation, which is used to design feedback controllers for structural systems, was combined with well-known stability results for scalar, first-order DDEs to determine delay properties for a first-order, linear system of equations. The major contribution of the paper is the straightforward method to approximate the maximum allowable delay for an n-dimensional system, and we have specifically aimed to quantify the stability bounds without solving the DDE.

The remainder of the paper is organized as follows. Background on DDEs is presented in Sec. II. Section III presents the stability analysis for a first-order, scalar DDE, and the results presented in that section enable the subsequent investigation of delay properties for n-dimensional, linear systems. Section IV describes the method of determining the maximum allowable delay for an n-dimensional system of equations by using a modal-coordinate transformation to diagonalize the $2n$ first-order, closed-loop equations of motion. This approach enables the use of some of the well-known DDE results in the literature. The application of the developed theory to a formation control problem is described in Sec. V, where two different control laws based upon defined communication structures are presented. Simulation results demonstrating the theory are also presented, followed by conclusions in Sec. VI.

II. Delay Differential Equations

Delay differential equations model systems with delay, and the literature over the past several decades has focused on analyzing the stability of this specific type of differential equation. Driver describes a DDE as a "differential equation with a retarded argument", that is, a DDE expresses some derivative of x, $x^{(n)}$, at time t as a function of $(x, \dot{x}, \ldots, x^{(n-1)})$ evaluated at time t and earlier instants[17].

There are two stability concepts in the analysis of DDEs: delay-independent and delay-dependent stability. Whereas delay-independent stability holds for all positive, finite delays, delay-dependent stability only holds for some values of the delays and instabilities occur when the delays are outside of the stability bounds [18–20]. In the case of linear, time-invariant DDEs, delay-independent stability criteria can be determined quite simply; however, determining bounds on delays becomes more challenging owing to the need to solve a transcendental equation, which has an infinite number of solutions.

Frequency-domain methods are one approach described in the literature to analyze stability of DDEs. In the case of linear, autonomous DDEs, the roots of the transcendental characteristic function are difficult to determine, which led researchers to explore other means of analyzing the stability of DDEs. Analytical methods using Pontryagin's theorem (for a single delay or a commensurable number of delays) are used to determine the number of zeros in the right-half plane, and the method of D subdivision can be applied to find the regions where the characteristic function has roots in the right-half plane as a function of the system parameters [18,21]. Mori et al. examined asymptotic stability of linear DDEs of the form $\dot{\boldsymbol{x}}(t) = A\boldsymbol{x}(t) + B\boldsymbol{x}(t - \tau)$, and results in the form of linear matrix inequalities (LMIs) provide both delay-independent and delay-dependent criteria [19,20]. Niculescu investigated necessary and sufficient conditions for delay-independent and delay-dependent stability using a matrix-pencil technique[22].

Time-domain methods can also be used to show delay-independent or delay-dependent stability using an extension of Lyapunov's second method for time-delay systems [17,18]. Driver describes the Lyapunov–Krasovskiĭ method as seeking to find a Lyapunov functional that includes information regarding the delay size, and then Lyapunov's second method can be carried through to determine stability. Dugard and Verriest show that asymptotic stability can be shown using a Lyapunov–Krasovskiĭ functional that leads to the delay Riccati equation[18]. Chopra and Spong have demonstrated delay-independent stability for networked passive systems with delays on the transmitted system outputs [23,24].

Additionally, some numerical methods have been developed recently to find stability regions in the time-delay parameter space. Kalmàr-Nagy presents a method to estimate the delay-dependent stability chart using a polynomial approximation of the transcendental characteristic equation[25]. Sipahi and Olgac have developed a method to find stability regions for multiple time-delay systems using a root-clustering technique, which finds the delay regions where the roots of the transcendental characteristic equation cross the imaginary axis into the right-half plane [26–28]. The work of Asl and Ulsoy [29,30] and Yi and Ulsoy[31] and the references therein are especially important to the work presented in this paper. Their focus is on a Lambert-function technique that is used to approximate the solution of a system of linear DDEs.

In all of the aforementioned methods, there are challenges in determining the delay-dependent bounds for large-dimensional systems with delays, such as solving LMIs, finding an appropriate Lyapunov–Krasovskiĭ function, or requiring extensive, problem-specific computation. The stability results for a scalar, first-order system with delay are well known, and this simplified model is exploited in this paper to determine approximate delay-dependent stability bounds for a multidimensional, linear system of equations subject to delays in the feedback control.

III. Stability Results for a Scalar, First-Order DDE

In this section we present some known results for a scalar, first-order DDE. Consider the DDE given below

$$\dot{x}(t) = ax(t) + bx(t-\tau) \tag{1}$$

Here, τ is a constant delay. In the parameter space, $S(0)$ is the set (a, b) where Eq. (1) is asymptotically stable for $\tau = 0$[18]. Thus, $S(0)$ is easily determined

$$S(0) = \{(a, b) : a + b < 0\} \tag{2}$$

Assume that $a < 0$, and using a Lyapunov–Krasovskiĭ approach, the conditions on b can be found such that (a, b) corresponds to the delay-independent set S_∞. A Lyapunov functional is defined as shown below

$$V(t) = x^2(t) + |a| \int_{t-\tau}^{t} x^2(s)\,\mathrm{d}s \tag{3}$$

A time-derivative of $V(t)$ reveals the condition for b

$$\begin{aligned}\dot{V}(t) &= 2x(t)\left[ax(t) + bx(t-\tau)\right] + |a|\left[x^2(t) - x^2(t-\tau)\right] \\ &= -|a|x^2(t) - |a|x^2(t-\tau) + 2bx(t)x(t-\tau) \\ &\leqslant (-|a| + |b|)\left[x^2(t) + x^2(t-\tau)\right]\end{aligned} \tag{4}$$

Therefore, delay-independent stability is achieved for $a \leqslant -|b|$

$$S_\infty = \{(a, b) : a + b < 0, a \leqslant -|b|\} \tag{5}$$

The delay-dependent set is complementary to S_∞ within $S(0)$[18].

$$S_\tau = \{(a, b) : a + b < 0, b < -|a|\} \tag{6}$$

To find the stability bound in the delay-dependent region for a delay τ, the transcendental characteristic equation from Eq. (1) is formed

$$s - a - be^{-s\tau} = 0 \tag{7}$$

By substituting $s = j\omega$ and expanding using Euler's identity, the real and imaginary parts of the characteristic equation can be written as shown

$$-a - b\cos(\omega\tau) = 0; \qquad \omega + b\sin(\omega\tau) = 0 \tag{8}$$

Hale[32] and Smith[33] show that the stable region, where the roots of the transcendental equation in Eq. (7) have $Re(s) < 0$, is the open region bounded by the curves $b = -a$ and the solution to Eq. (8) for $0 < \omega < \pi/\tau$. Figure 1

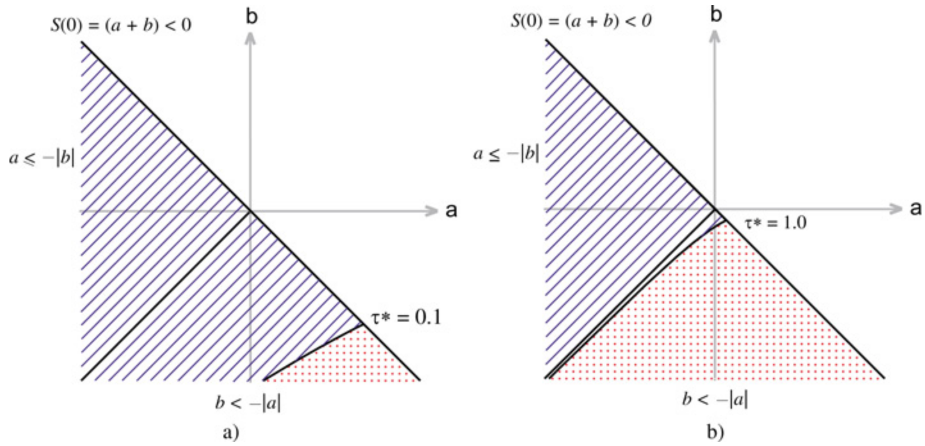

Fig. 1 Delay-independent and dependent stability regions for $\dot{x}(t) = ax(t) + bx(t - \tau)$.

shows the delay-independent and delay-dependent stability regions for Eq. (1) in the $(a(\omega), b(\omega))$ space for the range $0 < \omega < \pi/\tau$ and with $\tau = 0.1$ and $\tau = 1.0$. The asymptotically stable regions are the cross-hatched areas, and the unstable regions in $S(0)$ are dotted. From the above results, the stability bound on τ can be determined for any parameter set (a, b) in the delay-dependent region

$$\tau^* = \frac{\cos^{-1}(-a/b)}{\sqrt{b^2 - a^2}} \tag{9}$$

IV. Time-Delay Analysis

The objective is to determine the maximum system delay for n-dimensional, linear equations of motion. Assume that the second-order closed-loop equations for a coupled system can be written in a structural form: $M\ddot{z}(t) + C\dot{z}(t) + Kz(t) = 0$, where M, C, and K are $n \times n$ mass, damping, and stiffness matrices, respectively[34]. A first-order form can be derived for $\mathbf{Z}(t) = [z(t)\ \dot{z}(t)]^T$

$$\dot{\mathbf{Z}}(t) = \left[\begin{array}{c|c} 0_{n\times n} & I_{n\times n} \\ \hline -M^{-1}K & -M^{-1}C \end{array}\right] \mathbf{Z}(t) = A_{\rm cl}\mathbf{Z}(t) \tag{10}$$

This paper specifically examines closed-loop systems that have the linear, first-order form in Eq. (10). Here $A_{\rm cl}$ is an $2n \times 2n$ matrix and $\mathbf{Z}(t)$ is an $2n \times 1$ vector of generalized coordinates and their rates. Suppose that $\mathbf{Z}(t)$ is subject to some delay, τ, owing to some measurement, actuation, communication, or operator delay on the feedback states. It is assumed that this delay also acts on the kinematics to simplify the first-order, closed-loop form to the expression shown below

$$\dot{\mathbf{Z}}(t) = A_{\rm cl}\mathbf{Z}(t - \tau) \tag{11}$$

If $A_{\rm cl}$ is a diagonalizable matrix, a modal transformation of the following form can be chosen[34].

$$z(t) = \Phi\boldsymbol{\eta}(t); \qquad z(\cdot) = \Phi\boldsymbol{\eta}(\cdot) \tag{12}$$

Here, Φ is an $2n \times 2n$ matrix of the eigenvectors of $A_{\rm cl}$. Substituting Eq. (12) into the closed-loop form in Eq. (11) and multiplying by Φ^{-1} yields the following $2n$ first-order differential equations with delay

$$\dot{\boldsymbol{\eta}}(t) = A_{\rm d}\boldsymbol{\eta}(t - \tau) \tag{13}$$

The matrix $A_d = \Phi^{-1} A_{cl} \Phi$ is diagonal; therefore, the modal transformation decouples the matrix DDE in the η coordinates

$$\dot{\eta}_1(t) = \lambda_1 \eta_1(t - \tau_1)$$
$$\dot{\eta}_2(t) = \lambda_2 \eta_2(t - \tau_2)$$
$$\vdots$$
$$\dot{\eta}_{2n}(t) = \lambda_{2n} \eta_{2n}(t - \tau_{2n}) \tag{14}$$

The coefficients λ_i in the above equations are the eigenvalues of the closed-loop matrix, A_{cl}. Therefore, the coefficients can be real or complex. A stable closed-loop matrix will have eigenvalues with negative real parts.

For the case where the coefficients are real, the delay-independent and delay-dependent stability of the closed-loop system can be analyzed using the results presented in Sec. II for each scalar first-order DDE in Eq. (14). In the modal form above, the coefficient a in Eq. (1) is zero, which implies that the system is delay-independently stable for $b = \lambda_i = 0$ only. From the delay-dependent results for the optimal bound on the delay, the following relationship for each first-order DDE is derived

$$\tau_i^* = \frac{\pi}{2|\lambda_i|} \tag{15}$$

In the case that the coefficients are complex, the transcendental equation in Eq. (7) can be rewritten with $a = 0$ and b complex.

$$s - (b_R + jb_I)\, e^{-s\tau} = 0 \tag{16}$$

Here, b_R and b_I are the real and imaginary parts of b, respectively. The optimal bound on τ can be derived by substituting $s = j\omega$ into Eq. (16) and expanding using Euler's identity.

$$\tau_i^* = \frac{\tan^{-1}(-b_R/b_I)}{\sqrt{b_R^2 + b_I^2}} \tag{17}$$

This equation is a general expression for the DDE with $a = 0$ and b either real or complex. If $b_I = 0$, this expression is equivalent to that shown in Eq. (15).

The optimal bounds for each DDE in Eq. (14) can be computed using the general form in Eq. (17), and the smallest τ_i^* is the maximum allowable delay for the closed-loop system. At the maximum allowable delay, the system displays marginally stable behavior; for delays less than the maximum delay, the DDEs are asymptotically stable; and if the maximum delay is exceeded, the system will be unstable. Thus, delay bounds can be determined for a general closed-loop control form by solving an eigenvalue problem to diagonalize the closed-loop matrix. Stability bounds can be found without solving or approximating the solution of the DDE, which is contrasted with work by Asl and Ulsoy [29,30], and Yi and Ulsoy [31].

V. Application to Formation Control

The development in Sec. IV was used to determine the maximum allowable system delay for a coupled, n-dimensional system. In this section, the theory is applied to the formation control of a five-vehicle system. First, the formation-control problem and the vehicle model are presented. Based upon the form and properties of the vehicle model, expressions are derived for the error dynamics that govern the spacing between vehicles in the formation. Two control forms are explored based upon the decentralized communication structure between adjacent vehicles in the formation. The first control form uses a leader–follower communication structure, where each vehicle receives information from its preceding vehicle. The second form uses a bidirectional communication structure in which each vehicle receives state information from both its preceding and trailing vehicles.

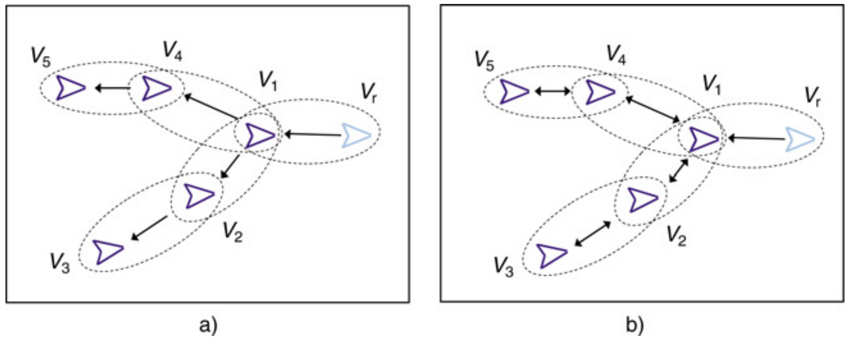

Fig. 2 Examples of communication structures in decentralized multi-vehicle formation control[9]. a) and b) show leader–follower and bidirectional communication structures, respectively.

A. Problem Definition

The decentralized formation-control problem for a five-vehicle system is shown in Fig. 2. Each vehicle pair is denoted by the dashed lines, and communication flow is shown by the arrows between vehicles. Figure 2a shows the leader–follower communication structure. This structure can be explored by considering the second vehicle V_2; V_2 receives state information from its lead V_1, and V_3 receives information from V_2. The first vehicle, V_1, will be referred to as the formation lead, which tracks a reference trajectory denoted here as an imaginary reference vehicle V_r. Figure 2b shows the bidirectional communication structure. In this communication structure, the formation lead receives information from the reference trajectory and both trailing vehicles, V_2 and V_4, and V_2 receives information from both V_1 and V_3.

B. Vehicle Model and Error Dynamics

The chosen vehicle model is a commonly used nonlinear kinematics model that represents a vehicle with zero or negligible velocity in the direction perpendicular to the vehicle's heading

$$\begin{aligned} \dot{x} &= v\cos\psi \\ \dot{y} &= v\sin\psi \\ \dot{\psi} &= \omega \end{aligned} \tag{18}$$

Here, x and y are the vehicle's inertial position in the two-dimensional (2-D) plane, v is the velocity in the direction of motion, ψ is the heading angle relative to the x axis, and ω is the angular turn rate of the vehicle. The velocity and angular turn rate are assumed to be the control inputs to the vehicle.

The vehicle model is differentially flat with flat outputs x and y[35]. Owing to the differential-flatness property, the state ψ and the two control inputs can be written as functions of the flat outputs and their derivatives as shown below

$$\begin{aligned} v &= \sqrt{\dot{x}^2 + \dot{y}^2} \\ \psi &= \tan^{-1}\left(\frac{\dot{y}}{\dot{x}}\right) \\ \omega &= \frac{\ddot{y}\dot{x} - \dot{y}\ddot{x}}{v^2} \end{aligned} \tag{19}$$

The second derivatives of the flat outputs are the highest derivatives that appear in the controls, v and ω. Therefore, new control inputs were defined as $(\ddot{x}, \ddot{y}) = (u, w)$. This transformation enables the nonlinear system in Eq. (18) to be represented as uncoupled double integrators.

$$\begin{bmatrix} \dot{x} \\ \dot{y} \\ \ddot{x} \\ \ddot{y} \end{bmatrix} = \begin{bmatrix} 0 & 0 & 1 & 0 \\ 0 & 0 & 0 & 1 \\ 0 & 0 & 0 & 0 \\ 0 & 0 & 0 & 0 \end{bmatrix} \begin{bmatrix} x \\ y \\ \dot{x} \\ \dot{y} \end{bmatrix} + \begin{bmatrix} 0 & 0 \\ 0 & 0 \\ 1 & 0 \\ 0 & 1 \end{bmatrix} \begin{bmatrix} u \\ w \end{bmatrix} \tag{20}$$

Thus, the control-law design is made easier by the transformation to the linear representation, which provides an exact linear model rather than a linear approximation [11,35].

The design focus is on the internal stability of the formation, that is, the ability to achieve and maintain a desired formation. Error variables are defined between the vehicle pairs as shown below. Note that the defined errors are in the x direction only. Owing to the uncoupled nature of the equations of motion, the development is identical in the y direction

$$e_1 = x_r - x_1 - d_1; \quad \dot{e}_1 = \dot{x}_r - \dot{x}_1; \quad \ddot{e}_1 = \ddot{x}_r - \ddot{x}_1 = \ddot{x}_r - u_1 \tag{21}$$

$$e_i = x_1 - x_i - d_i; \quad \dot{e}_i = \dot{x}_1 - \dot{x}_i; \quad \ddot{e}_i = \ddot{x}_1 - \ddot{x}_i = u_1 - u_i; \quad i = 2, 4 \tag{22}$$

$$e_i = x_{i-1} - x_i - d_i; \quad \dot{e}_i = \dot{x}_{i-1} - \dot{x}_i; \quad \ddot{e}_i = \ddot{x}_{i-1} - \ddot{x}_i = u_{i-1} - u_i; \quad i = 3, 5 \tag{23}$$

In Eq. (21), the formation lead tracks a desired reference trajectory, x_r, at some constant distance, d_1. Equation (22) is the relative error between vehicles 1 and 2 and vehicles 1 and 4 separated by some desired distance, and Eq. (23) follows similarly for vehicles 3 and 5.

C. Control-Law Development

1. *Leader–Follower Communication Structure*

For the leader–follower communication structure, a form for the control input to the ith vehicle u_i is assumed as shown below. Initially, the control input did not include delay in the measured or communicated state information. Note that the control laws for vehicles 1, 2, and 3 are designed independently of the control laws for vehicles 1, 4, and 5 owing to the nature of the leader–follower communication structure

$$u_i = k_i e_i + c_i \dot{e}_i + \ddot{x}_r \tag{24}$$

The closed-loop error dynamics have the following form for vehicles 1, 2, and 3

$$\begin{bmatrix} \dot{e}_1 \\ \dot{e}_2 \\ \dot{e}_3 \\ \ddot{e}_1 \\ \ddot{e}_2 \\ \ddot{e}_3 \end{bmatrix} = \begin{bmatrix} 0 & 0 & 0 & 1 & 0 & 0 \\ 0 & 0 & 0 & 0 & 1 & 0 \\ 0 & 0 & 0 & 0 & 0 & 1 \\ -k_1 & 0 & 0 & -c_1 & 0 & 0 \\ k_1 & -k_2 & 0 & c_1 & -c_2 & 0 \\ 0 & k_2 & -k_3 & 0 & c_2 & -c_3 \end{bmatrix} \begin{bmatrix} e_1 \\ e_2 \\ e_3 \\ \dot{e}_1 \\ \dot{e}_2 \\ \dot{e}_3 \end{bmatrix} \tag{25}$$

From the closed-loop equations, the characteristic equation and the eigenvalues are easily determined

$$\prod_{i=1}^{3} \left[s^2 + c_i s + k_i \right] = 0 \Rightarrow \lambda_{i_{1,2}} = -\frac{c_i}{2} \pm \frac{\sqrt{c_i^2 - 4k_i}}{2} \tag{26}$$

If the closed-loop eigenvalues have negative real parts, the multivehicle system is asymptotically stable. The closed-loop eigenvalues are found similarly for the platoon of vehicles 1, 4, and 5. Therefore, control gains in Eq. (24) can be selected to yield stable formation convergence.

To find the maximum allowable delay in this closed-loop system, it is assumed that the error terms in the control input have a constant delay τ

$$u_i = k_i e_i(t - \tau) + c_i \dot{e}_i(t - \tau) + \ddot{x}_r \tag{27}$$

The error dynamics can be written using the control input form with delay, where A_{cl} is equal to the matrix in Eq. (25). Following with the development in Sec. IV, it is assumed that the delay also acts on the kinematics in order to write the closed-loop form below

$$\dot{\boldsymbol{e}}(t) = A_{\mathrm{cl}}\boldsymbol{e}(t - \tau) \tag{28}$$

If A_{cl} is diagonalizable, the modal transformation described in Sec. IV can be applied to find six scalar, first-order DDEs from which the optimal bound on the delay can be determined for each equation. Thus, the maximum allowable delay for the system can be determined. However, for this closed-loop form, A_{cl} is diagonalizable only if there are six distinct eigenvalues, which cannot be achieved if all of the control gains in Eq. (24) are equal. The "diagonalizability" of the closed-loop matrix can be described by the condition number of the Φ matrix. Large condition numbers indicate that a diagonal form of A_{cl} cannot be found as Φ is not invertible. The next section describes a communication structure where equal control gains are not problematic in the diagonalizability of A_{cl}.

2. Bidirectional Communication Structure

In the bidirectional communication structure, control laws for vehicles 1, 2, and 3 cannot be designed independently of control laws for vehicles 1, 4, and 5. From Fig. 2(b), it can be seen that the first vehicle is affected by both the second and fourth vehicles, which couples the two vehicle platoons. Control inputs of the form shown below are assumed

$$\begin{aligned} u_1 &= k\,(e_1 - e_2 - e_4) + c\,(\dot{e}_1 - \dot{e}_2 - \dot{e}_4) + \ddot{x}_r \\ u_i &= k\,(e_i - e_{i+1}) + c\,(\dot{e}_i - \dot{e}_{i+1}) + \ddot{x}_r; \qquad i = 2, 4 \\ u_i &= k\,(e_i) + c\,(\dot{e}_i) + \ddot{x}_r; \qquad i = 3, 5 \end{aligned} \tag{29}$$

The control inputs result in motion similar to physically placing springs and dampers between the vehicles in the x and y directions; therefore, the bidirectional communication structure is structurally analogous to a mass-spring-damper system linked as shown in Fig. 2(b). Again, the closed-loop error dynamics can be written to evaluate stability. The error vector and closed-loop matrix, A_{cl}, are defined below for this control form.

$$\boldsymbol{e} = \begin{bmatrix} e_1 & e_2 & e_3 & e_4 & e_5 & \dot{e}_1 & \dot{e}_2 & \dot{e}_3 & \dot{e}_4 & \dot{e}_5 \end{bmatrix}^T \tag{30}$$

$$A_{\mathrm{cl}} = \left[\begin{array}{c|c} 0_{5\times5} & I_{5\times5} \\ \hline -K & -C \end{array}\right] \tag{31}$$

$$K = \begin{bmatrix} k & -k & 0 & -k & 0 \\ -k & 2k & -k & k & 0 \\ 0 & -k & 2k & 0 & 0 \\ -k & k & 0 & 2k & -k \\ 0 & 0 & 0 & -k & 2k \end{bmatrix}; \qquad C = \begin{bmatrix} c & -c & 0 & -c & 0 \\ -c & 2c & -c & c & 0 \\ 0 & -c & 2c & 0 & 0 \\ -c & c & 0 & 2c & -c \\ 0 & 0 & 0 & -c & 2c \end{bmatrix} \tag{32}$$

Whereas the eigenvalues for this system do not have a concise analytical form as those in Eq. (26), the closed-loop system will be stable for positive definite stiffness and damping matrices.

As in the development of the delayed leader–follower control law, a constant delay, τ, is assumed in the feedback control laws

$$\begin{aligned} u_1 &= k\,[e_1(t-\tau) - e_2(t-\tau) - e_4(t-\tau)] + c\,[\dot{e}_1(t-\tau) - \dot{e}_2(t-\tau) - \dot{e}_4(t-\tau)] + \ddot{x}_r \\ u_i &= k\left[e_i(t-\tau) - e_{i+1}(t-\tau)\right] + c\left[\dot{e}_i(t-\tau) - \dot{e}_{i+1}(t-\tau)\right] + \ddot{x}_r; \qquad i = 2, 4 \\ u_i &= k\,[e_i(t-\tau)] + c\,[\dot{e}_i(t-\tau)] + \ddot{x}_r; \qquad i = 3, 5 \end{aligned} \tag{33}$$

Again, assuming delays in the kinematics, the closed-loop error dynamics can be written in the form $\dot{\boldsymbol{e}}(t) = A_{\mathrm{cl}}\boldsymbol{e}(t-\tau)$. Because the stiffness and damping matrices are symmetric, A_{cl} is diagonalizable for equal gains in the control inputs to the individual vehicles[34].

D. Simulation Results

Simulation results are presented below to illustrate the application of the theories in Secs. IV and V to a five-vehicle, formation-control problem governed by the two control-law forms described above. Numerical results were simulated using a fourth-order Runge–Kutta solver with initial conditions held constant until the determined optimal bound, τ. For example, the governing equations of motion in the x direction can be described as shown below, where $\boldsymbol{x} = [x_1\ x_2\ x_3\ x_4\ x_5]^T$

$$\ddot{\boldsymbol{x}}_i(t) = u_i\,(t, \boldsymbol{x}_i(t-\tau), \dot{\boldsymbol{x}}_i(t-\tau))\,; \qquad \boldsymbol{x}_i(t) = \boldsymbol{x}_i(0), \quad \dot{\boldsymbol{x}}_i(t) = \dot{\boldsymbol{x}}_i(0), \quad -\tau \leqslant t \leqslant 0 \tag{34}$$

Whereas delays in the kinematics are assumed in the derivation of the maximum allowable delay, the simulations assume zero delay in the kinematic equations.

Four sets of simulation results are presented:

1) Leader–follower control law with nominal gains $c = 6$ and $k = 16$. As described previously, the closed-loop equations are not diagonalizable if the gains are not distinct. In this case, the gains for the vehicles are: $c_1 = 6$ and $k_1 = 16$, $c_2 = c_4 = 7$ and $k_2 = k_4 = 16$, and $c_3 = c_5 = 5$ and $k_3 = k_5 = 16$. For these gains and control structure, the closed-loop matrix, A_{cl} has complex eigenvalues.
2) Leader–follower control law with nominal gains $c = 16$ and $k = 6$. Again, in this case the gains cannot be distinct. The vehicle gains are: $c_1 = 16$ and $k_1 = 6$, $c_2 = c_4 = 17$ and $k_2 = k_4 = 6$, and $c_3 = c_5 = 15$ and $k_3 = k_5 = 6$. Thus, the closed-loop error dynamics has real eigenvalues.
3) Bidirectional control law with gains $c = 6$ and $k = 16$. For this control form, the gains can be identical, and these gains lead to four real and six imaginary eigenvalues for A_{cl}.
4) Bidirectional control law with gains $c = 16$ and $k = 6$. Here, A_{cl} has ten real eigenvalues.

Figures 3–6 show the formation convergence for the four sets of results. Note that the vehicles are traveling from left to right in the figure, and each vehicle has initial position and velocity errors. The first vehicle in the formation tracks a reference trajectory with a constant velocity in the x direction where $\dot{x}_r = 1$ distance unit/time unit (DU/TU). In each figure, the top, left subplot shows the formation convergence without delay in the feedback control law; the

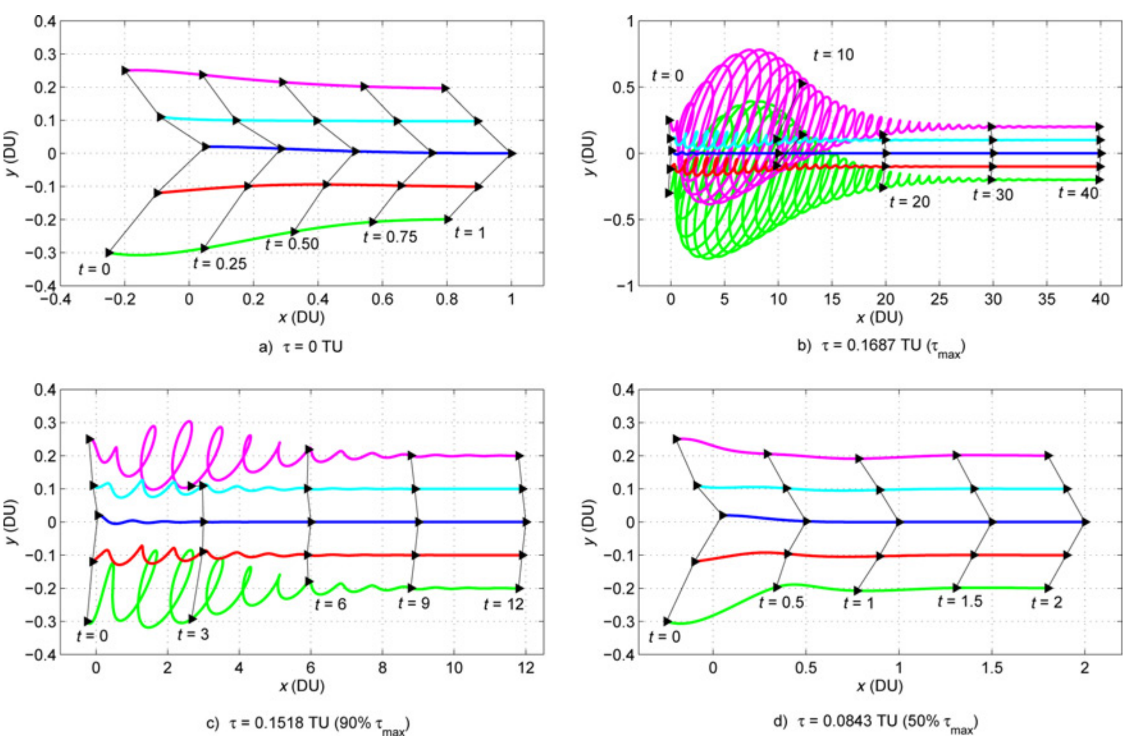

Fig. 3 Formation results for the leader–follower communication structure ($c = 6$, $k = 16$).

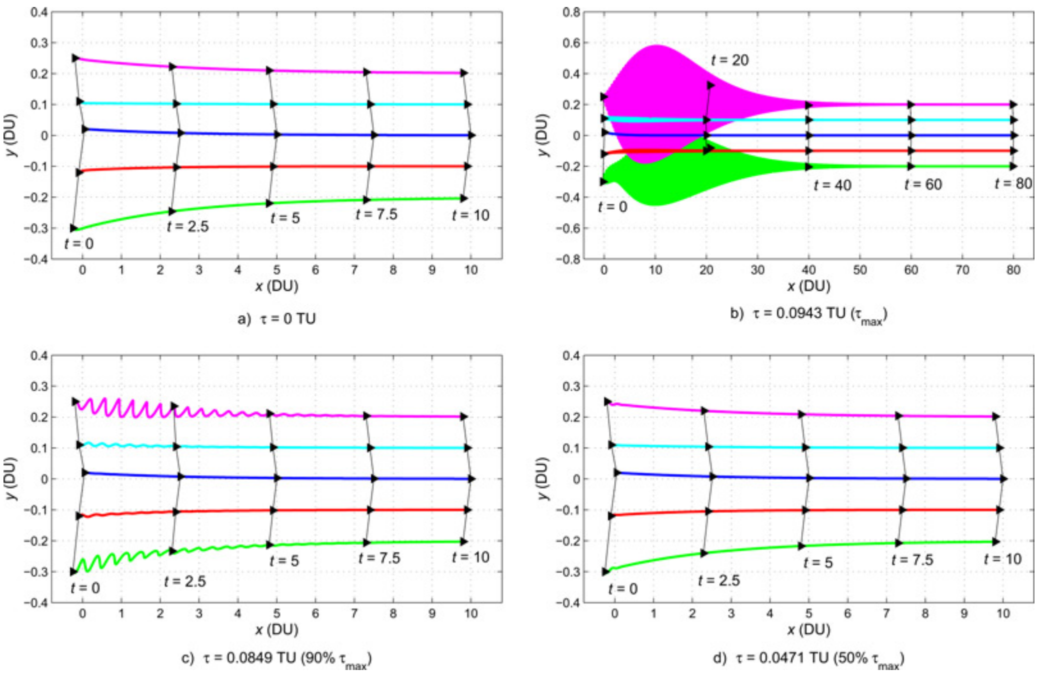

a) τ = 0 TU
b) τ = 0.0943 TU (τ_{max})
c) τ = 0.0849 TU (90% τ_{max})
d) τ = 0.0471 TU (50% τ_{max})

Fig. 4 Formation results for the leader-follower communication structure ($c = 16$, $k = 6$).

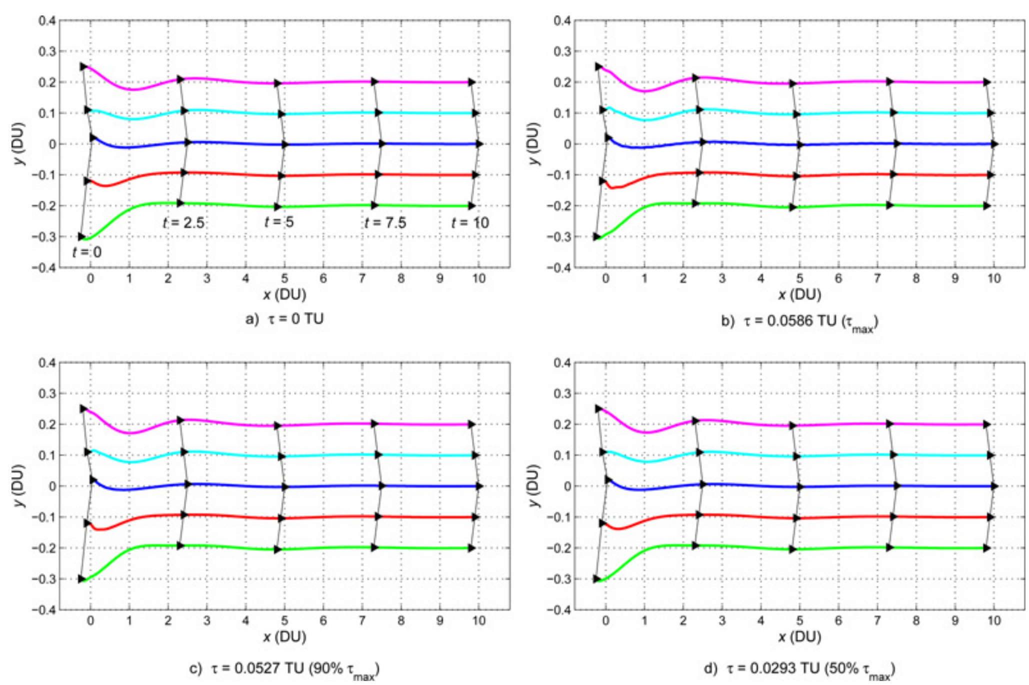

a) τ = 0 TU
b) τ = 0.0586 TU (τ_{max})
c) τ = 0.0527 TU (90% τ_{max})
d) τ = 0.0293 TU (50% τ_{max})

Fig. 5 Formation results for the bidirectional communication structure ($c = 6$, $k = 16$).

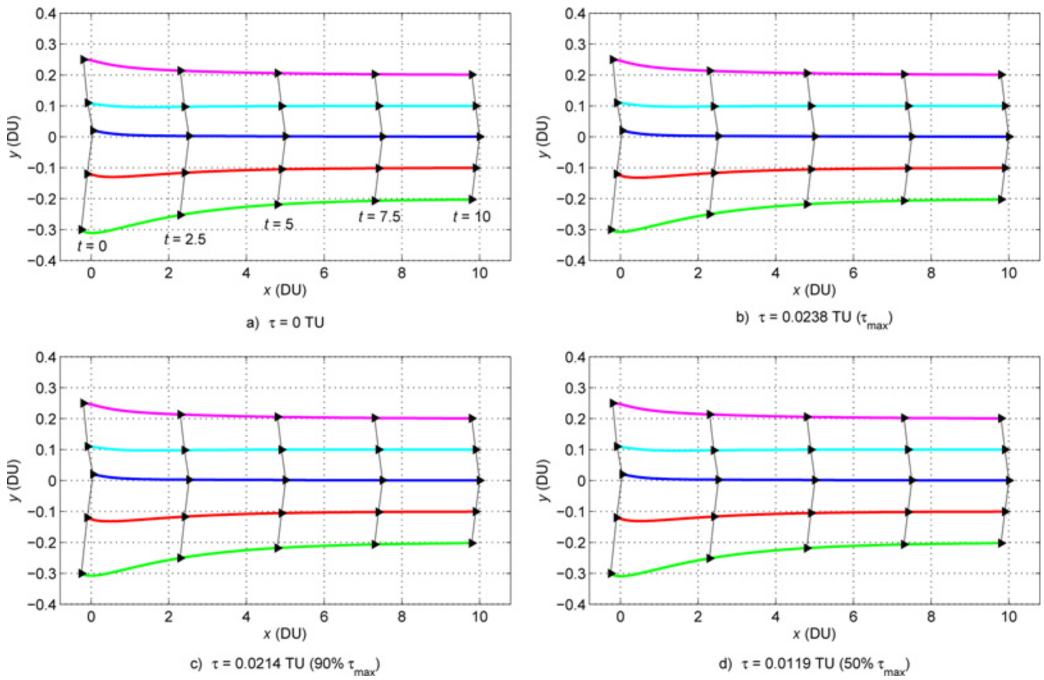

Fig. 6 Formation results for the bidirectional communication structure ($c = 16$, $k = 6$).

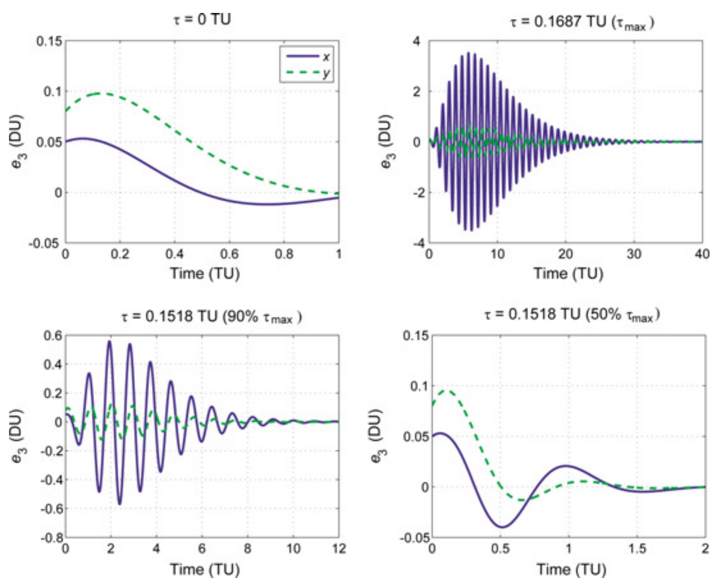

Fig. 7 Error convergence of the third vehicle for the leader-follower communication structure ($c = 6$, $k = 16$).

top, right subplot shows the formation convergence for the maximum allowable delay in the system determined from Eq. (17); in the bottom, left subplot, the delay has been reduced to 90% of the maximum delay; and in the bottom, right subplot, the delay has been decreased to half of the maximum allowable delay. Formation geometry is denoted at various times during the simulation to show the evolution of formation convergence. Figures 7–10 show the error convergence of V_3 in the formation in both the x and y directions for the same delays as in the previous figures.

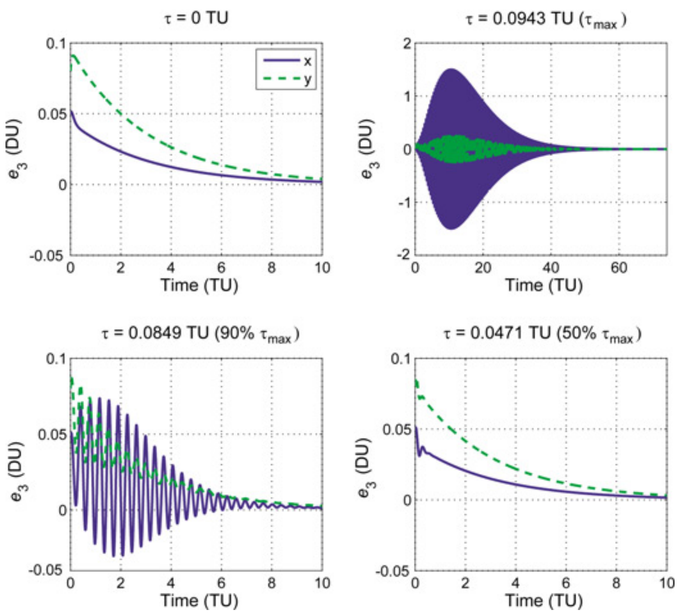

Fig. 8 Error convergence of the third vehicle for the leader-follower communication structure ($c = 16$, $k = 6$).

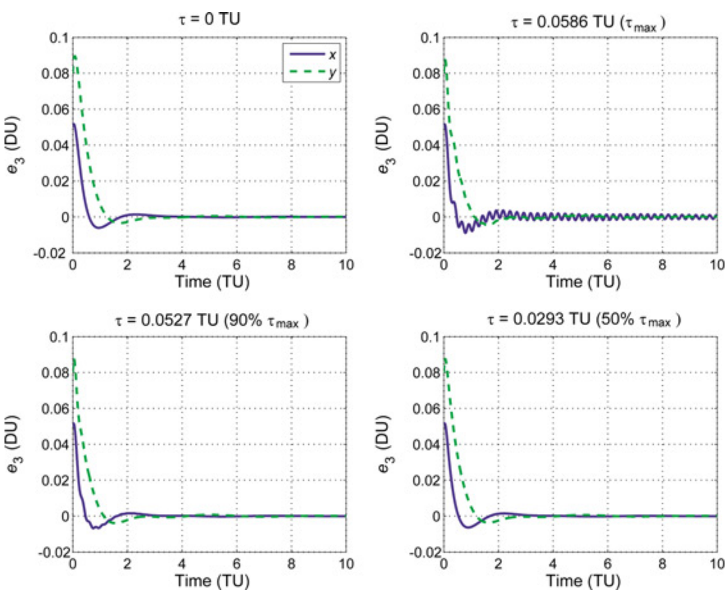

Fig. 9 Error convergence of the third vehicle for the bidirectional communication structure ($c = 6$, $k = 16$).

Results are summarized in Table 1, where the formation convergence time is defined as the time when all five vehicles are within 10% of their desired separation in both the x and y directions.

Several conclusions can be drawn from both the figures and the table. The formation convergence for the systems simulated with the maximum allowable delay exhibits highly oscillatory behavior, as expected, near the stability bounds. In the results for the leader–follower control laws, the convergence time increases significantly when the delay is near the optimal bound. Decreasing the maximum delay by half greatly improves the convergence results as is evident in both the formation figures and the third-vehicle figures. The leader–follower communication structure is

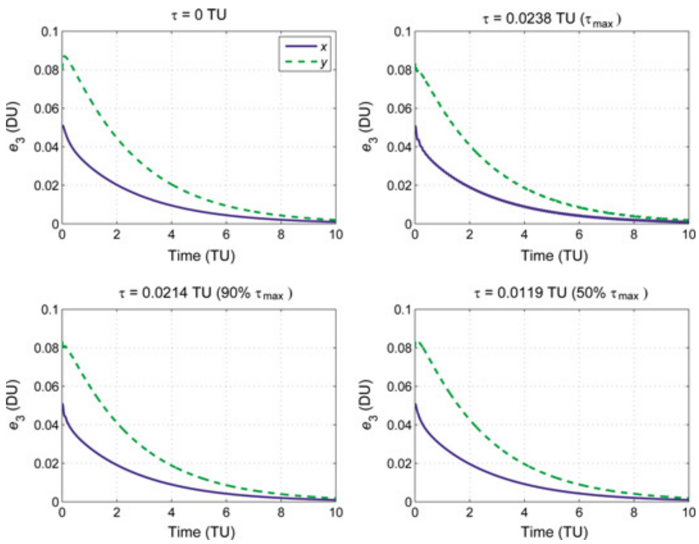

Fig. 10 Error convergence of the third vehicle for the bidirectional communication structure ($c = 16$, $k = 6$).

Table 1 Control-law convergence and error results

Communication structure	Gains	Time-delay (TU)	Convergence time (TU)
Leader–follower	$c = 6, k = 16$	0	0.8620
		0.1687 (τ_{max})	39.9728
		0.1518 ($0.9\tau_{max}$)	11.4032
		0.0843 ($0.5\tau_{max}$)	1.5646
Leader–follower	$c = 16, k = 6$	0	7.0300
		0.0943 (τ_{max})	73.2709
		0.0849 ($0.9\tau_{max}$)	9.2813
		0.0471 ($0.5\tau_{max}$)	6.4791
Bidirectional	$c = 6, k = 16$	0	1.5800
		0.0586 (τ_{max})	7.1912
		0.0527 ($0.9\tau_{max}$)	1.6211
		0.0293 ($0.5\tau_{max}$)	1.6077
Bidirectional	$c = 16, k = 6$	0	5.8400
		0.0238 (τ_{max})	5.6520
		0.0214 ($0.9\tau_{max}$)	5.6327
		0.0119 ($0.5\tau_{max}$)	5.7254

less robust in terms of the large oscillations that were induced in the outside vehicles (V_3 and V_5), as the inputs to these vehicles contain the errors of the preceding vehicles. The oscillations become more localized for the bidirectional communication structure, and the effect of this localization is evident in the convergence times in the table. In both communication structures, some filtering techniques may lessen the effects of the delay. In the bidirectional structure the control gains were chosen to be equal, which does not require the control designer to be concerned with the diagonalizablity of the closed-loop equations as is the case in the leader–follower form. Therefore, the bidirectional form has two advantages over the leader–follower form: robustness to time-delay effects and diagonalizability for equal gains.

E. Discussion

The theory presented here can be summarized as an approach to determine delay-dependent stability bounds for a coupled, closed-loop system. This approach does not support the determination of delay-independent bounds. Because the kinematics are assumed delayed to diagonalize the system, the coefficients a_i are equal to zero in Eq. (14), which places the scalar DDE coefficients in the delay-dependent stability region of Fig. 1.

Additionally, the results can be compared to previously referenced work by Chopra and Spong, where delay-independent stability was demonstrated for passive systems using a Lyapunov analysis [23,24]. That result was demonstrated using a circular communication structure where the feedback coupling had equal gains and time delays impacted transmitted states only. Whereas these results could also apply to the passive dynamics of the vehicle model in Eq. (18), it remains to be seen whether a Lyapunov function can be determined for the specific formation control laws presented here, which have unequal control gains, delays on both transmitted and measured states, and are developed for a noncircular communication structure.

The approach to quantify stability bounds has reduced the computational analysis to essentially solving an eigenvalue value problem in order to diagonalize, or decouple, the closed-loop equations of motion. This approach is contrasted with the analytical rigor of finding a Lyapunov function for each control law or the computational challenges in implementing some of the previously discussed work in Sec. II.

VI. Conclusions

In this paper, a straightforward method is presented for determining the maximum allowable time delay in a linear, n-dimensional system using some well-known results from the literature on DDEs. Using a modal-coordinate transformation, the system of linear, first-order equations of motion can be decoupled into scalar, first-order DDEs. This theory is applied to a multivehicle, decentralized formation-control problem, from which two control schemes are developed based upon the desired communication structure of the formation. Simulation results demonstrate the stability and performance of the formation convergence when delays are within the calculated stability bounds. Additionally, the effects of communication structure become evident in the formation convergence when delays are introduced. The approach presented in this paper reduces the problem of determining delay-dependent stability bounds to an eigenvalue problem, which eliminates the rigor of other approaches that require finding a problem-specific Lyapunov function, solving LMIs, or solving computationally expensive root-finding problems.

Future work includes the inverse problem where control laws are designed to accommodate expected time delays in the state feedback. Desired or expected system delays lead to closed-loop eigenvalues; however, the closed-loop eigenvectors must also be chosen appropriately to arrive at feedback gains that meet the communication-structure constraints.

Acknowledgments

Research funding was provided by the Lindbergh/Lycoming Grant administered by the Charles A. and Anne Morrow Lindbergh Foundation. Research funding was also provided by the National Science Foundation Graduate Research Fellowship. Any opinions, findings, conclusions, or recommendations expressed in this document are those of the author and do not necessarily reflect the views of the National Science Foundation.

The authors would also like to thank Dr. Kalmàr-Nàgy and the reviewers for their insightful comments on the paper.

References

[1] Swaroop, D., and Hedrick, J. K., "String Stability of Interconnected Systems," *IEEE Transactions on Automatic Control*, Vol. 41, No. 3, 1996, pp. 349–357.
doi: 10.1109/9.486636

[2] Swaroop, D., and Hedrick, J. K., "Constant Spacing Strategies for Platooning in Automated Highway Systems," *ASME Journal of Dynamic Systems, Measurement, and Control*, Vol. 21, No. 3, September 1999, pp. 462–470.

[3] Swaroop, D., and Rajagopal, K. R., "A Review of Constant Time Headway Policy for Automatic Vehicle Following," *Proceedings of the 2001 IEEE Intelligent Transportation Systems Conference*, Institute of Electrical and Electronics Engineers, New York, NY, 2001, pp. 65–69.

[4] Barooah, P., and Hespanha, J. P., "Error Amplification and Disturbance Propagation in Vehicle Strings with Decentralized Linear Control," *Proceedings of the 44th IEEE Conference on Decision and Control, and the European Control Conference*, Institute of Electrical and Electronics Engineers, New York, NY, 2005, pp. 4964–4969.

[5] Lohr, G. W., Oseguera-Lohr, R. M., Abbott, T. S., and Capron, W. R., "Flight Evaluation of a Time-Based Airborne Inter-Arrival Spacing Tool," *5th USA/Europe ATM R&D Seminar*, Eurocontrol, Budapest, Hungary, June 2003, Electronic proceedings available at: http://atm2003.eurocontrol.fr/papers_calendar.

[6] Barmore, B., Abbott, T., and Krishnamurthy, K., "Airborne-Managed Spacing in Multiple Arrival Streams," *24th International Congress of the Aeronautical Sciences*, Yokohama, Japan, September 2004, Electronic proceedings available at: http://www.csun.edu/∼serl/Articles/airborne%20managed%20spacing.pdf

[7] Pallotino, L., Feron, E. M., and Bicchi, A., "Conflict Resolution Problems for Air Traffic Management Systems Solved with Mixed Integer Programming," *IEEE Transactions on Intelligent Transportation Systems*, Vol. 3, No. 1, 2002, pp. 3–11.
doi: 10.1109/6979.994791

[8] Jackson, M. R. C., Sharma, V., Haissig, C. M., and Elgersma, M., "Airborne Technology for Distributed Air Traffic Management," *44th IEEE Conference on Decision and Control, and the European Control Conference 2005*, Institute of Electrical and Electronics Engineers, New York, NY, 2005, pp. 3947–3954.

[9] Stipanović, D. M., İnalhan, G., Teo, R., and Tomlin, C. J., "Decentralized Overlapping Control of a Formation of Unmanned Aerial Vehicles," *Automatica*, Vol. 40, August 2004, pp. 1285–1296.

[10] Chen, C.-T., *Linear System Theory and Design*, Oxford University Press, New York, NY, 1999, Chap. 8, Sec. 4.

[11] Weitz, L. A., Hurtado, J. E., and Sinclair, A. J., "Decentralized Cooperative-Control Design for Multivehicle Formations," *Journal of Guidance, Control, and Dynamics*, Vol. 31, No. 4, 2008, pp. 970–979.
doi: 10.2514/1.33009.

[12] Gu, Y., Seanor, B., Campa, G., Napolitano, M. R., Rowe, L., Gururajan, S., and Wan, S., "Design and Flight Testing Evaluation of Formation Control Laws," *IEEE Transactions on Control Systems Technology*, Vol. 14, No. 6, 2006, pp. 1105–1112.
doi: 10.1109/TCST.2006.880203

[13] Siljak, D. D., *Decentralized Control of Complex Systems*, Academic, New York, NY, 1991, Chap. 9.

[14] Olfati-Saber, R., and Murray, R. M., "Consensus Problems in Networks for Agents with Switching Topology and Time-Delays," *IEEE Transactions on Automatic Control*, Vol. 49, No. 9, 2004, pp. 1520–1533.
doi: 10.1109/TAC.2004.834113

[15] Subbarao, K., and Muralidhar, P., "Cooperative Control of UAVs in Dynamic Pursuit Subject to Communication Delays," *Proceedings of the AIAA Guidance, Navigation, and Control Conference*, San Francisco, CA, August 2005.

[16] Dionne, D., and Rabbath, C. A., "Real-Time Decentralized Pursuer-Evader Assignment for Cooperating UCAVs Using the DTC Algorithm," *Proceedings of the AIAA Guidance, Navigation, and Control Conference*, AIAA, Reston, VA, 2007, AIAA paper No. 2007-6454.

[17] Driver, R. D., *Ordinary and Delay Differential Equations*, Springer-Verlag, New York, NY, 1977, Chap. 5.

[18] Dugard, L., and Verriest, E. I., *Stability and Control of Time-Delay Systems*, Springer-Verlag, London, 1998, Chap. 1.

[19] Mori, T., "Criteria for Asymptotic Stability of Linear Time-Delay Systems," *IEEE Transactions on Automatic Control*, Vol. 30, No. 2, 1985, pp. 158–161.
doi: 10.1109/TAC.1985.1103901

[20] Mori, T., and Kokame, H., "Stability of $\dot{x}(t) = Ax(t) + Bx(t - \tau)$," *IEEE Transactions on Automatic Control*, Vol. 34, No. 4, 1989, pp. 460–462.
doi: 10.1109/9.28025

[21] Kolmanovskii, V. B., and Nosov, V. R., *Stability of Functional Differential Equations*, Academic International Press, Orlando, FL, 1986, Chap. 3.2.

[22] Niculescu, S.-I., "Stability and hyperbolicity of linear systems with delayed state: a Matrix-Pencil Approach," *Institute for Mathematics and its Applications: Journal of Mathematical Control & Information*, Vol. 15, 1998, pp. 331–347.
doi: 10.1093/imamci/15.4.331

[23] Chopra, N., and Spong, M. W., "Synchronization of Networked Passive Systems with Time Delays and Application to Bilateral Teleoperation," *Proceedings of the Society of Instrumentation and Control Engineering of Japan Annual Conference*, Okayama, Japan, August 2005.

[24] Chopra, N., and Spong, M. W., "Passivity-Based Control of Multi-Agent Systems," *Advances in Robot Control: From Everyday Physics to Human-Like Movements*, edited by S. Kawamura and M. Svinin, Springer-Verlag, Berlin, Germany, 2006, pp. 107–134.

[25] Kalmàr-Nagy, T., "A New Look at the Stability Analysis of Delay Differential Equations," *Proceedings of the ASME International Design Engineering Technical Conferences and the Computers and Information in Engineering Conferences*, American Society of Mechnical Engineers, Fairfield, NJ, 2005.

[26] Sipahi, R., and Olgac, N., "Degenerate Cases in Using the Direct Method," *ASME Journal of Dynamic Systems, Measurement, and Control*, Vol. 125, No. 2, 2003, pp. 194–201.
doi: 10.1115/1.1567756

[27] Sipahi, R., and Olgac, N., "A Novel Stability Study on Multiple Time-Delay Stability, (MTDS) Using the Root Clustering Paradigm," *Proceedings of the 2004 American Control Conference*, American Automatic Control Council, Boston, MA, 2004, pp. 5422–5427.

[28] Sipahi, R., and Olgac, N., "Complete Stability Robustness of Third-Order LTI Multiple Time-Delay Systems," *Automatica*, Vol. 41, No. 8, 2005, pp. 1413–1422.

[29] Asl, F. M., and Ulsoy, A. G., "Analytical Solution of a System of Homogeneous Delay Differential Equations via the Lambert Function," *Proceedings of the American Control Conference*, American Automatic Control Council, Chicago, IL, 2004, pp. 2496–2500.

[30] Asl, F. M., and Ulsoy, A. G., "Analysis of a System of Linear Delay Differential Equations," *American Society of Mechanical Engineers Journal of Dynamic Systems, Measurement, and Control*, Vol. 125, No. 2, 2003, pp. 215–223.
doi: 10.1115/1.1568121

[31] Yi, S., and Ulsoy, A. G., "Solution of a System of Linear Delay Differential Equations Using the Matrix Lambert Function," *Proceedings of the American Control Conference*, American Automatic Control Council, Minneapolis, MN, 2006, pp. 2433–2438.

[32] Hale, J., *Theory of Function Differential Equations*, Springer–Verlag, New York, NY, 1977, Chap. 5, Appendix: Stability of Characteristic Equations.

[33] Smith, H., "MAT 598 Applied Delay Differential Equations," *Lecture Notes: Arizona State University*, 2004, pp. 45–50, http://math.la.asu.edu/%7Ehalsmith/FDE.pdf [retrieved October 2007].

[34] Junkins, J. L., and Kim, Y., *Introduction to Dynamics and Control of Flexible Structures*, AIAA, Washington, DC, 1993, Chap. 3.

[35] Murray, R. M., Rathinam, M., and Sluis, W., "Differential Flatness of Mechanical Control Systems: A Catalog of Prototype Systems," *Proceedings of the 1995 ASME International Mechanical Engineering Congress and Expo*, American Society of Mechanical Engineers, Fairfield, NJ, 1995.

Ella Atkins
Associate Editor